

Supporting Information

2-(2'-Hydroxyphenyl)-benzothiazole (HBT)-quinoline conjugate: Highly specific fluorescent probe for Hg²⁺ based on ESIPT and its application in bioimaging

Sunanda Sahana^a, Gargi Mishra^b, Sri Sivakumar^b, Parimal K. Bharadwaj^{a*}

^aDepartment of Chemistry, Indian Institute of Technology Kanpur, Kanpur-208016, India

^bDepartment of Chemical Engineering, Indian Institute of Technology Kanpur, Kanpur-208016, India

Contents

| | |
|--|---------|
| Fig. S1. ¹ H NMR spectrum of A | Page S2 |
| Fig. S2. ¹³ C NMR spectrum of A | Page S2 |
| Fig. S3. ESI MS spectrum of the A | Page S3 |
| Fig. S4. ¹ H NMR spectrum of B | Page S3 |
| Fig. S5. ¹³ C NMR spectrum of B | Page S4 |
| Fig. S6. ESI MS spectrum of the B | Page S4 |
| Fig. S7. ¹ H NMR spectrum of L | Page S5 |
| Fig. S8. ¹³ C NMR spectrum of L | Page S5 |
| Fig. S9. ESI MS spectrum of the L | Page S6 |
| Fig. S10 ESI MS spectrum of the L – Hg ²⁺ complex | Page S6 |
| Fig. S11 Absorbance titration of L with increasing Hg ²⁺ ion | Page S7 |
| Fig. S12 Job's plot | Page S7 |
| Fig. S13 Plot for detection limit | Page S8 |
| Table 1: Comparison of some ESIPT based Hg ²⁺ sensors | Page S8 |

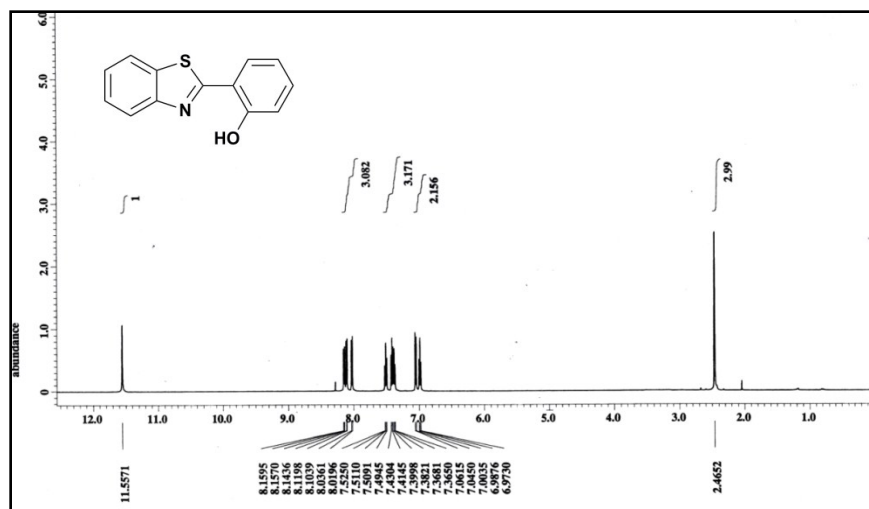


Fig.S1 ¹H NMR spectrum of A

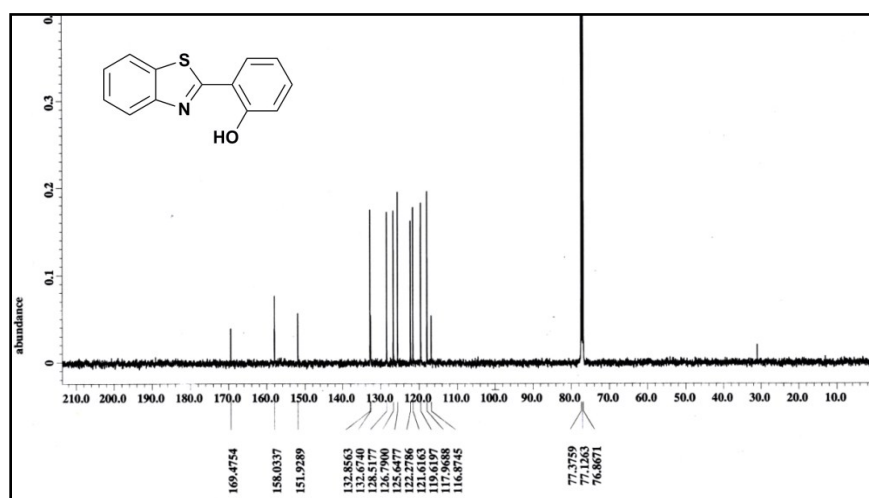


Fig.S2 ¹³C NMR spectrum of A

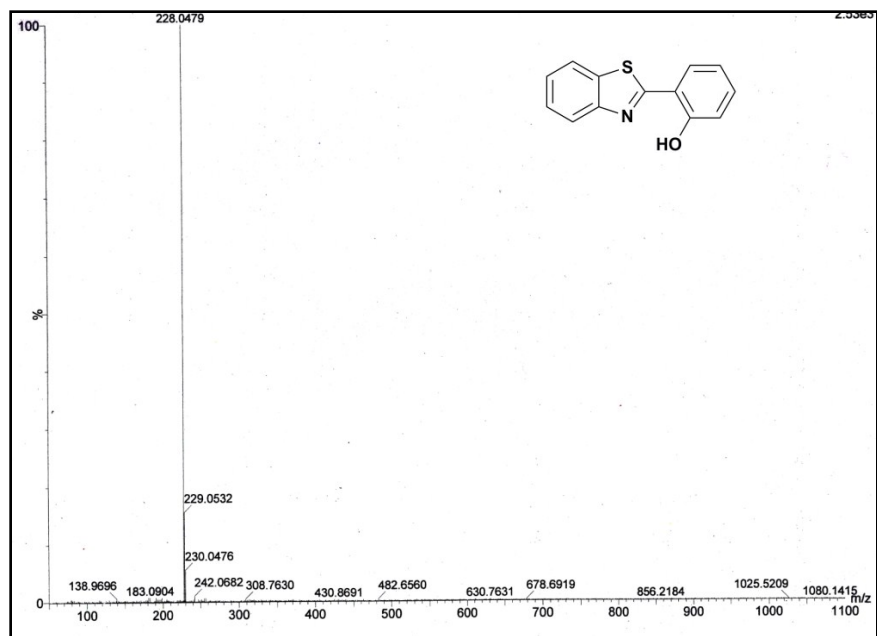


Fig. S3 ESI MS spectrum of the A

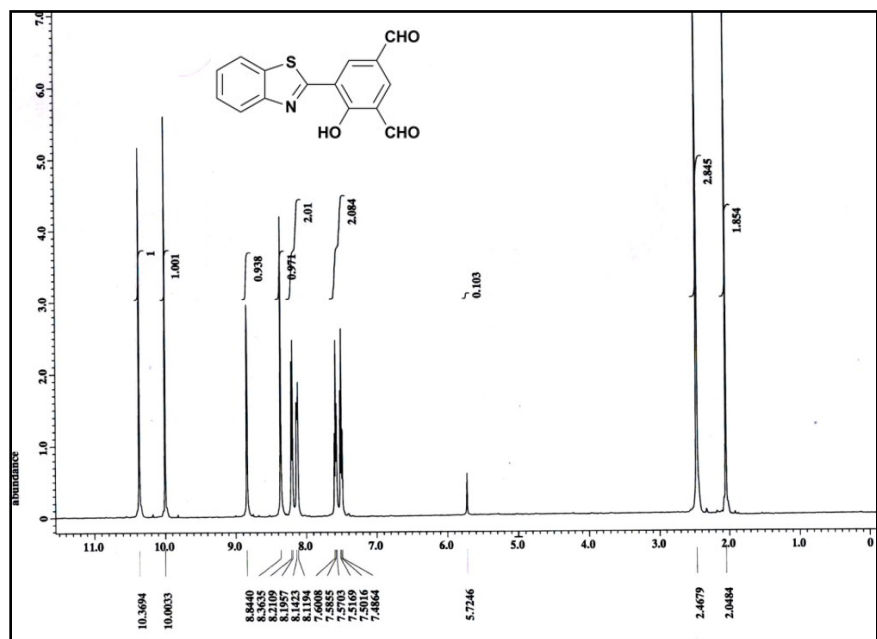


Fig. S4 ¹H NMR spectrum of B

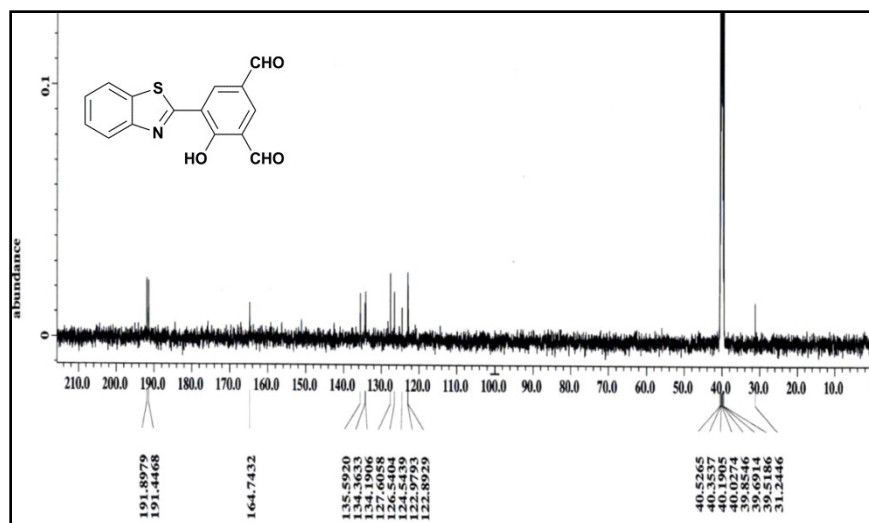


Fig. S5 ^{13}C NMR spectrum of B

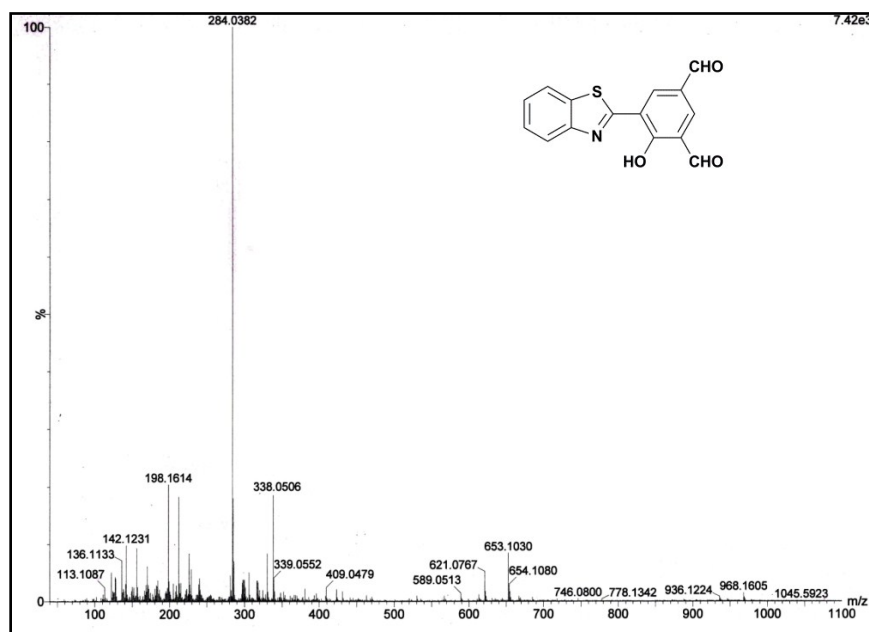


Fig. S6 ESI MS spectrum of the B

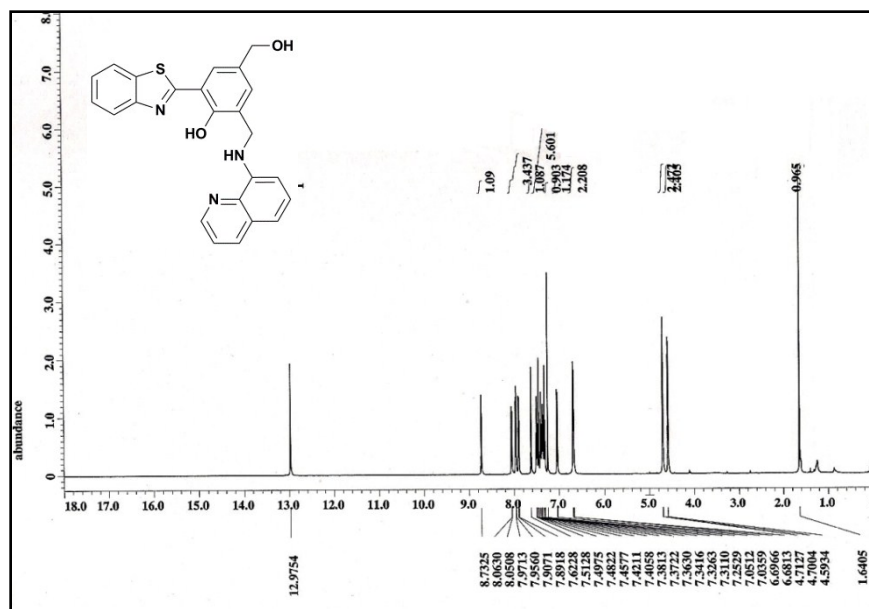


Fig. S7 ¹H NMR spectrum of **L**

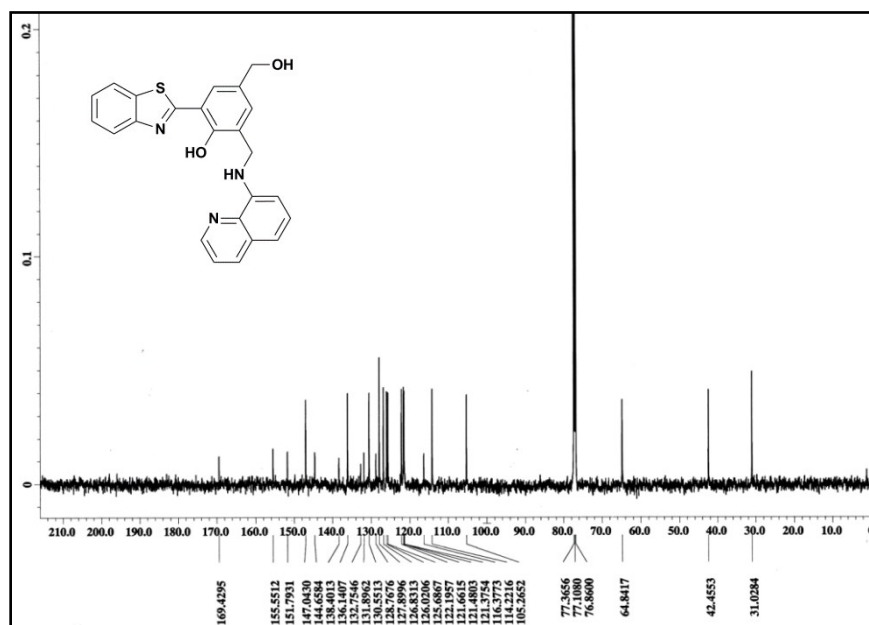


Fig. S8 ¹³C NMR spectrum of **L**

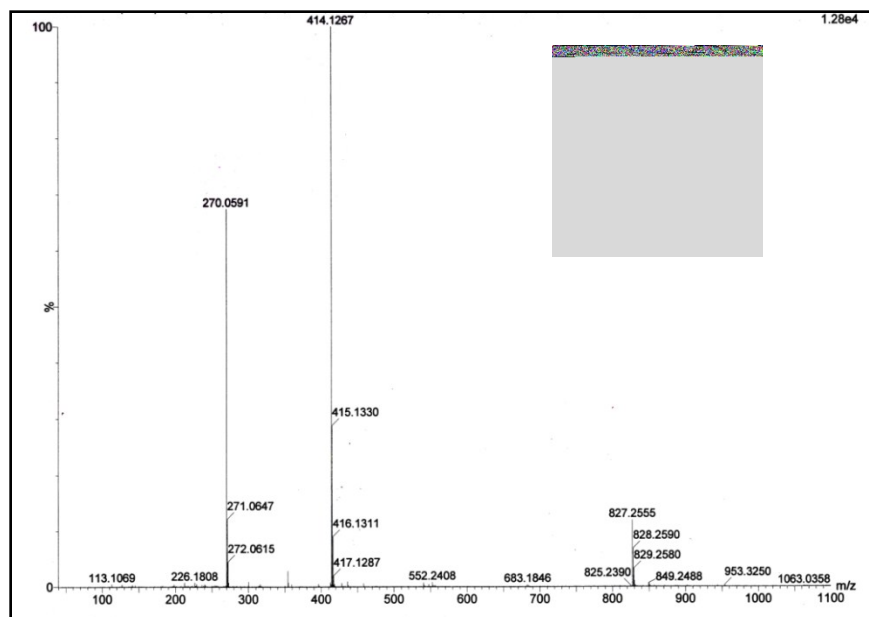


Fig. S9 ESI MS spectrum of the L

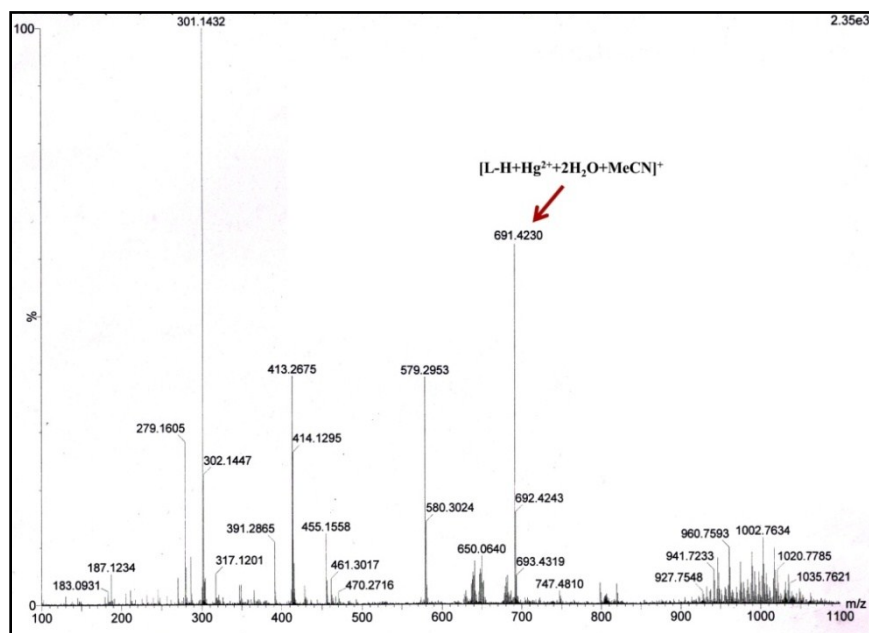


Fig. S10 ESI MS spectrum of the L – Hg²⁺ complex

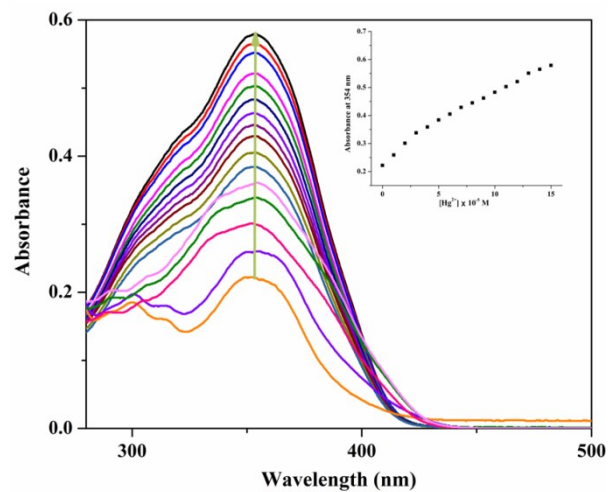


Fig. S11 Absorbance titration of **L** with increasing Hg²⁺ ion concentration in MeCN: H₂O (3:2, v/v, 10 mM HEPES Buffer, pH = 7). $\lambda_{\text{exc}} = 340 \text{ nm}$. Arrow indicates the increasing trend in Hg²⁺ ion concentration.

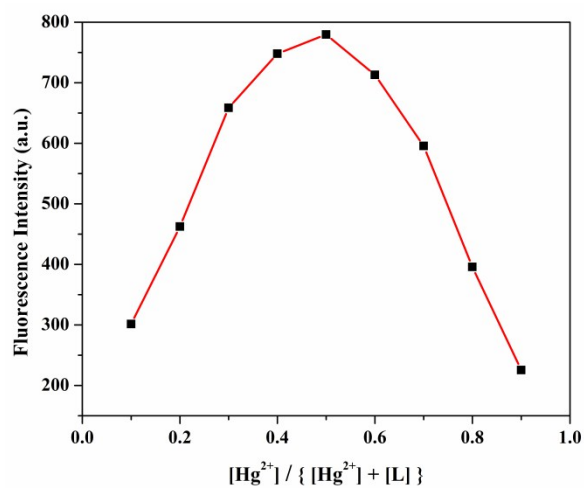


Fig. S12 Job's plot for determination of binding stoichiometry between **L** and Hg²⁺

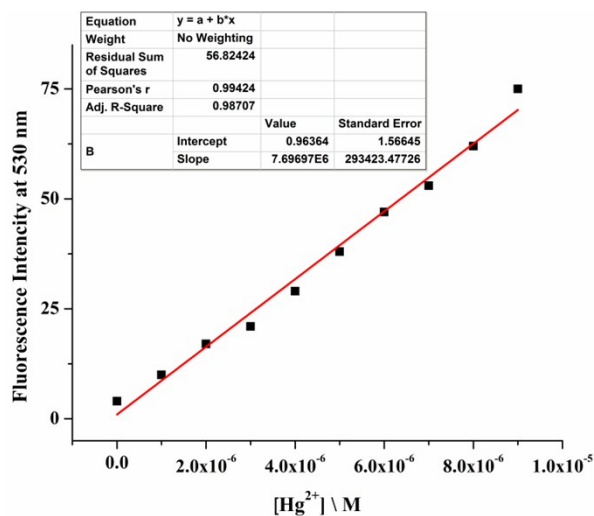


Fig.S13 Linear response curve of **L** at 590 nm depending on the Hg^{2+} ion concentration for determination of lowest detection limit

| Entry | Probe | Solvent system | Detection limit | Binding constant | Stoichiometry (Ligand: Hg^{2+}) | Imaging applied on cells | References |
|-------|----------|---|--------------------|-----------------------------------|---|----------------------------------|---------------|
| 1 | 2 | $\text{CH}_3\text{CN}/\text{H}_2\text{O}$ (1:1; V/V) | - | $1.04 \times 10^5 \text{ M}^{-2}$ | 2:1 | - | 1 |
| 2 | 1 | PBS buffer (~1% CH_3CN) | 20 ppb | - | 2:1 | - | 2 |
| 3 | 1 | PBS buffer (0.5% CH_3CN) | 5.1 nM | - | 1:1 | <i>HeLa</i> cells | 3 |
| 4 | 2 | PBS buffer (0.5% CH_3CN) | 3.8 nM | - | 1:1 | <i>HeLa</i> cells | 3 |
| 5 | PDP | $\text{CH}_3\text{CN}/\text{H}_2\text{O}$ (1 : 1;V/V) | 4.9 μM | $7.5 \times 10^3 \text{ M}^{-1}$ | 1:1 | lung cancer cell line (NCI-H460) | 4 |
| 6 | Pvi | PBS buffer (1% CH_3CN) | 7.8 nM | - | - | <i>HeLa</i> cells | 5 |
| 7 | L | $\text{CH}_3\text{CN}:\text{H}_2\text{O}$ (3:2; V/V) | 0.11 μM | $1.24 \times 10^4 \text{ M}^{-1}$ | 1:1 | <i>HeLa</i> cells | Present Study |

Table 1: Comparison of some ESIPT based Hg^{2+} sensors

References

1. A. Misra and M. Shahid, *J. Phys. Chem. C.*, 2010, **114**, 16726-16739.
2. M. Santra, B. Roy, and K. H. Ahn, *Org. Lett.*, 2011, **13**, 3422-3425.
3. W. Luo, H. Jiang, K. Zhang, W. Liu, X. Tang, W. Dou, Z. Ju, Z. Li and W. Liu, *J. Mater. Chem. B.*, 2015, **3**, 3459-3464.
4. S. Goswami, S. Maity, A. C. Maity, A.K. Das, B. Pakhira, K. Khanra, N. Bhattacharyya and S. Sarkar, *RSC Adv.*, 2015, **5**, 5735-5740.
5. B. Gu, L. Huang, N. Mi, P. Yin, Y. Zhang, X. Tu, X. Luo, S. Luo and S. Yao, *Analyst.*, 2015, **140**, 2778-2784.